Bulletin of Volcanology (2018) 80: 9
https://doi.org/10.1007/s00445-017-1184-y

RESEARCH ARTICLE

A volcanic event forecasting model for multiple tephra records, demonstrated on Mt. Taranaki, New Zealand

Magret Damaschke[1] · Shane J. Cronin[1,2] · Mark S. Bebbington[1]

Received: 20 April 2017 / Accepted: 6 December 2017 / Published online: 20 December 2017

Abstract

Robust time-varying volcanic hazard assessments are difficult to develop, because they depend upon having a complete and extensive eruptive activity record. Missing events in eruption records are endemic, due to poor preservation or erosion of tephra and other volcanic deposits. Even with many stratigraphic studies, underestimation or overestimation of eruption numbers is possible due to mis-matching tephras with similar chemical compositions or problematic age models. It is also common to have gaps in event coverage due to sedimentary records not being available in all directions from the volcano, especially downwind. Here, we examine the sensitivity of probabilistic hazard estimates using a suite of four new and two existing high-resolution tephra records located around Mt. Taranaki, New Zealand. Previous estimates were made using only single, or two correlated, tephra records. In this study, tephra data from six individual sites in lake and peat bogs covering an arc of ~ 120° downwind of the volcano provided an excellent temporal high-resolution event record. The new data confirm a previously identified semi-regular pattern of variable eruption frequency at Mt. Taranaki. Eruption intervals exhibit a bimodal distribution, with eruptions being an average of ~ 65 years apart, and in 2% of cases, centuries separate eruptions. The long intervals are less common than seen in earlier studies, but they have not disappeared with the inclusion of our comprehensive new dataset. Hence, the latest long interval of quiescence, since ~ AD 1800, is unusual, but not out of character with the volcano. The new data also suggest that one of the tephra records (Lake Rotokare) used in earlier work had an old carbon effect on age determinations. This shifted ages of the affected tephras so that they were not correlated to other sites, leading to an artificially high eruption frequency in the previous combined record. New modelled time-varying frequency estimates suggest a 33–42% probability of an explosive eruption from Mt. Taranaki in the next 50 years, which is significantly lower than suggested by previous studies. This work also demonstrates some of the pitfalls to be avoided in combining stratigraphic records for eruption forecasting.

Keywords Tephra · Tephrostratigraphy · Probabilistic eruption forecasting · Mt. Taranaki · Weibull renewal · Hazard

Introduction

Improving hazard assessments with accurate probabilistic forecasts is an ongoing task, driven by high and increasing population densities around volcanoes across the world (Small and Naumann 2001). An unexpected large-scale eruption may trigger volcanic disasters (e.g. Krakatau 1882; Self and Rampino 1981; Mt. Pelee 1902; Tanguy 1994; Mt. Vesuvius AD79; Sheridan et al. 1981), but even 'small' eruptions (< 0.01 km^3 of pyroclastics), like that of Ruapehu (New Zealand) in 1995–1996, impact greatly on our increasingly more technological societies (Johnston et al. 2000). Long-term dormant volcanoes pose a significant compounding risk, because the risk is often underestimated by their inhabitants. For example, Pinatubo was dormant for 650 years prior to its devastating 1991 eruption (Dartevelle et al. 2002; Gaillard 2006), misleading the local population. Even with an increasing understanding of volcanic systems, many mafic to intermediate volcanoes with irregular reawakening eruption patterns remain inexplicably diverse in behaviour and poorly predictable (e.g. Miyaji 1988; Scandone et al. 1993; Melnik and Sparks 1999; Andreastuti et al. 2000). Robust eruption

Editorial responsibility: L. Sandri

✉ Magret Damaschke
damaschm@gmail.com

[1] Volcanic Risk Solutions, Massey University, Private Bag 11222, Palmerston North 4410, New Zealand

[2] School of Environment, University of Auckland, Private Bag 92019, Auckland 1142, New Zealand

forecasts at many volcanoes are hindered by a lack of well-documented volcanic histories. Event records that are long and detailed enough to enable identification of fundamental eruption recurrence patterns are rare.

In this study, a new and highly detailed eruption record extending back to 30,000 cal year BP was examined for Mt. Taranaki in order to test methods of probabilistic eruption forecasting. The most important feature of this new record was that it spans a wide dispersal arc around this volcano for the first time (Fig. 1). Previous studies (Turner et al. 2008, 2009) used one or two stratigraphic records to develop probabilistic forecasts, but this base data has been superseded in recent studies by Damaschke et al. (2017a), who added four new lake and peat tephra records. The distribution of these sampling sites around a ~ 120° northeast-southeast arc downwind of the volcano provides the opportunity to track the dominant tephra dispersal directions and also evaluate tephra preservation biases and variations between sites.

A well-constrained multiple-site event stratigraphy makes the overall eruption history record more representative and inclusive of the actual eruptive behaviour, providing a more robust basis for improved probabilistic hazard forecasts. Nevertheless, combining sequences from more than one site must be conducted with care, to avoid over- or under-estimating the true eruption frequency. This is in part due to self-similar chemical compositions making individual andesitic tephra bed correlation challenging (Cronin et al. 1996; Donoghue et al. 2007; Damaschke et al. 2017a, b). Statistical methods for correlating multiple records using radiocarbon age and stratigraphy are well demonstrated (Turner et al. 2009; Green et al. 2014), but the quality of the result depends on the accuracy of the age determinations. Particularly difficult is the matching of near-contemporaneous tephras, as well as situations where the sedimentation regime trapping tephra deposits is discontinuous, or highly variable between sites. These issues are addressed in this study and a new probabilistic eruption hazard forecast is presented for Mt. Taranaki. Further, this paper outlines how to avoid pitfalls during stratigraphic merging procedures in order to derive more reliable probabilistic eruption forecasts for periodically active volcanoes.

Eruption history of Mt. Taranaki

Mt. Taranaki is an andesitic stratovolcano located in the western North Island of New Zealand (Fig. 1). Its current period of dormancy has lasted for ~ 200 years (Platz et al. 2012). Volcanic activity is known from this centre for over 170,000 years, based on mass flow and tephra deposits on its lower flanks and ring-plain (Alloway et al. 1995, 2005; Turner et al. 2008, 2009, 2011a; Zernack et al. 2009, 2011). Alloway et al. (1995) estimated a sub-Plinian eruption frequency of one event per 330 years, based on post-32-ky tephra deposits, but implied that smaller-scaled eruptions were likely far more frequent. Taranaki-sourced tephras within distal lacustrine sediments have also been identified to the N-NE of the volcano, with one fall per 1.1 kyr identified in Waikato lakes (Lowe 1988), and one event per 1.4 kyr in Auckland palaeolakes (Shane 2005; Molloy et al. 2009). These also highly underestimate the underlying volcanic activity, because they only include the larger magnitude events that disperse ash up to 270 km and in a narrow specific wind direction to the

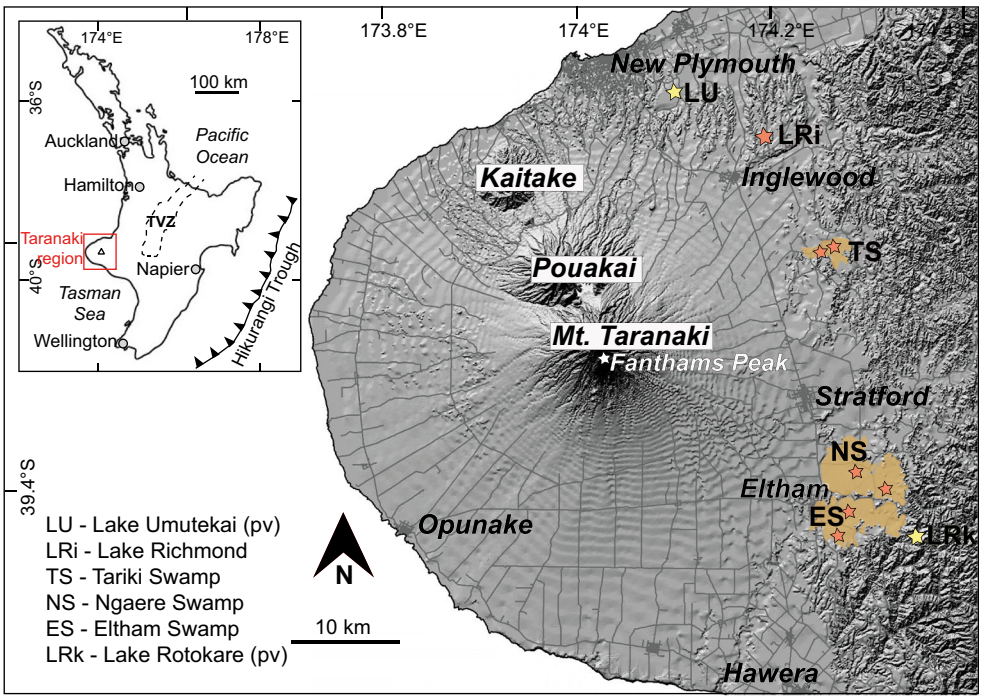

Fig. 1 Location map of the tephra deposition sites (pv = previous studied sites by Turner et al. 2008, 2009; highlighted in yellow), Cape Egmont, western North Island, New Zealand. Stars indicate specific coring locations. *TVZ* Taupo Volcanic Zone

NNE. The first temporal high-resolution tephrochronological studies at this volcano (Turner et al. 2008, 2009) identified a clear time-variability in eruptions, with semi-regular ~ 1500-year period cycles in eruption frequency noted over the past ~ 10 ky BP. Between the extremes of these cycles, there was a fivefold difference in the annual eruptive frequency of Mt. Taranaki. Based on a tephra record from sediments below Lake Umutekai, north-north-east of the volcano (Fig. 1), Turner et al. (2008) estimated a 37–48% chance of an eruption over the next 50 years. After combining these data with a second tephra record from a location southeast of the volcano (Lake Rotokare), some apparent gaps in the original eruption record were 'filled', leading Turner et al. (2009) to raise the 50-year probability for an eruption at Mt. Taranaki to 52–59%.

Approach and methods

Dataset—a new Mt. Taranaki tephrostratigraphy

A complete eruptive activity record is not achievable from a single stratigraphic section or core, due to the variability of preservation and wind dispersal of tephra from volcanoes. Here, we use a multiple-source temporal high-resolution eruption record recently obtained by Damaschke et al. (2017a), merged first by manual correlation and subsequently by a statistical matching approach. Damaschke et al. (2017a) recovered nine cores from four new deposition sites, including Lake Richmond, Eltham Swamp, Ngaere Swamp and Tariki Swamp, as well as combined those with two existing cores from Lake Umutekai and Lake Rotokare collected in earlier studies by Turner et al. (2008, 2009) (Fig. 1, Table 1).

Mineral layers within these sequences were sampled and primary tephras identified by optical microscopy and geochemical analyses. A small number of mineral layers were not classified as tephras, because they were dispersed within host sediment and/or showed diverse physical and geochemical characteristics (Damaschke et al. 2017a). Tephras in multiple cores from single sites were previously combined using chemical groupings, age-depth models and mineral/physical characteristics to produce six site-composite tephra records.

Table 1 Applied dataset obtained in previous studies by Damaschke et al. (2017a)

Tephra deposition site	Number of Taranaki-derived tephras encompassed in the composite record	Age range of the composite record (cal ky BP)
Lake Umutekai (LU)	103	1.4–11.5
Lake Richmond (LRi)	132	0.4–14.5
Tariki Swamp (TS)	64	1.7–17.4
Ngaere Swamp (NS)	68	1.8–13.4
Eltham Swamp (ES)	80	1.5–30
Lake Rotokare (LRk)	41	0.3–7

Individual tephra ages were estimated using vertically well-spaced radiocarbon dates in each core (Damaschke et al. 2017a) and modelling the age between these using a piecewise cubic Hermitian interpolating polynomial (Fritsch and Carlson 1980). Calibration was performed using OxCal Version 4.2 (Bronk Ramsey 2013) and the Southern Hemisphere SHCal13 atmospheric calibration curve (Hogg et al. 2013). A summary of the dataset used as the basis of this study is given in Table 1.

Temporal models for eruption occurrence

Several statistical models have been applied to model eruption histories. The simplest approach, used mainly with sparse datasets is a Poisson process (Wickman 1966; De la Cruz-Reyna 1991), where repose intervals are described by an exponential (memory-less) distribution. Hence, the rate of volcanic eruptions $\lambda(t)$ is a constant λ independent of time t. The probability of an eruption onset occurring in a short time interval $(t,\ t+\Delta)$ is approximately $\lambda\Delta$, and thus λ can be thought of as the instantaneous rate of occurrence.

A memory-less repose assumption does not fit when repose intervals are more complex and variable over time (Wickman 1966; Bebbington and Lai 1996a). Hence, Bebbington and Lai (1996a) introduced the Weibull renewal model. A renewal process depends on the inter-event time τ, rather than on the absolute time t. The inter-event times are independent and identically distributed according to a known probability density function $f(\tau)$. Hence, the time to the next event is dependent on the time since the last event (e.g. Reyment 1969; Bebbington and Lai 1996a; Bebbington 2010). The occurrence rate of a renewal process is given by:

$$\lambda(t) = \frac{f(t-s)}{1-F(t-s)}, \tag{1}$$

with $t - s = \tau$ as the elapsed repose time, hence,

$$\lambda(\tau) = \frac{f(\tau)}{1-F(\tau)}, \tag{2}$$

where the most recent event occurred at time $s < t$, and $f(\tau) = F(\tau)$' is the renewal density function. Marzocchi and Bebbington (2012) summarised a large number of renewal distribution functions used in volcanology, but that used here is the Weibull distribution, where:

$$f(\tau) = \alpha(\beta\tau)^{\alpha-1}\exp[-(\beta\tau)^{\alpha}], \alpha, \beta > 0, \tag{3}$$

with α and β being shape and scale parameters, respectively.

If $\alpha = 1$, the Weibull distribution reduces to an exponential distribution; if $\alpha < 1$, the model is 'over-dispersed', or shows clustering behaviour; and if $\alpha > 1$, the result is a semi-periodic

distribution with a mode at $\tau = (1/\beta)(1 - 1/\alpha)^{1/\alpha}$. The Weibull renewal process has been successfully fitted to historical eruption data from a large number of volcanoes (e.g. Bebbington and Lai 1996a, b; Cronin et al. 2001; Watt et al. 2007; Dzierma and Wehrmann 2010; Garcia-Aristizabal et al. 2012).

However, when the distribution of inter-event times is bimodal, a mixture of Weibull distributions may be more appropriate (Jiang and Murthy 1995, 1998; Turner et al. 2008):

$$f(\tau) = p\alpha_1\beta_1^{\alpha_1}\tau^{\alpha_1-1}\exp[-(\beta_1\tau)^{\alpha_1}] + (1-p)\alpha_2\beta_2^{\alpha_2}\tau^{\alpha_2-1}\exp[-(\beta_2\tau)^{\alpha_2}], \quad (4)$$

where $0 < p < 1$ is the mixing proportion, and the modes are at $\tau = \beta_1^{-1}(1-1/\alpha_1)^{1/\alpha_1}$ and $\tau = \beta_2^{-1}(1-1/\alpha_2)^{1/\alpha_2}$. Given any density function $f(\tau)$ and underlying inter-event times τ, the parameters can be estimated by maximising the log-likelihood:

$$logL(\tau) = \left[1-F\left(\tau^*\right)\right]\prod_{i=1}^{n} f(\tau_i), \quad (5)$$

where τ^* is the elapsed repose time since the last event and $\tau_1,\ldots, \tau_n$ are the inter-event times. Turner et al. (2008) used Monte Carlo simulation to model uncertainties associated with event ages and hence inter-event times. To determine the start of the observation period is effectively impossible; hence, observation is normally assumed to start at the first recorded eruption.

The method of moments or least squares are alternative techniques to estimate the parameters of a given distribution (Press et al. 1992; Bebbington and Lai 1996b; Boudt et al. 2011). A more serious issue than the calculation of parameter values is that of selecting the distribution that should be used. Distributions with more parameters, if they include a nested simpler model (for example, the exponential distribution contained in the Weibull), will always fit better. However, the more parameters used in any model, the higher the likelihood of overfitting. To evaluate which model best balances this bias-variance trade-off, the Akaike Information Criterion (AIC; Akaike 1977) can be applied, which measures the goodness of fit using:

$$\mathrm{AIC} = -2logL + 2k, \quad (6)$$

where k is the number of parameters and logL is the log-likelihood of the model. The model with the lower AIC value is favoured. Given any two estimated models, a difference of 1.5–2 in the AIC value is usually considered as significant (Akaike 1977).

Results

Eruption frequency records

Tephras recovered in lake and peat sediment cores surrounding Mt. Taranaki are our basis for understanding eruption rates. The time frame encapsulated by the records and the number of tephra layers preserved is not uniform across the cores (Fig. 2, Table 1). Estimates were thus made of the time-varying annual eruption rates over time at each single site with the use of a Gaussian kernel smoother (Silverman 1984, 1986; Wand and Jones 1994) with a bandwidth of 100 years, (Fig. 2a). However, integration across all sites is important, because one or two sites are likely to have little chance of recording all tephra falls due to variable wind and tephra dispersal patterns (Carey and Sparks 1986) and/or variations in eruption style and magnitude (Woods 1995; Bursik 1998).

At Lake Richmond, 129 Taranaki eruptions were recorded with an average interval of 113 years, similar to that found at Lake Umutekai (111 years). Both lakes show similar cyclical patterns of ~1000–1500-year-long periods with particularly high rates of tephra deposition (HRTD) centred at ~0.5, 2, 3.5, 5, 7, 8.5, 10.5 and 12.5 cal ky BP (indicated by numbers 1–8 in Fig. 2a), separated by intervals of low rates of tephra deposition (LRTD) and/or a lack of tephra deposition (both indicated by letters A-H in Fig. 2b). Older variations in the rate of tephra deposition are documented only within the Tariki Swamp record (HRTD intervals-9 and -10 at ~15 and 17 cal ky BP, respectively, separated by LRTD interval-I at ~16.5 cal ky BP; Fig. 2a, b).

The HRTD interval-1 (~0.5 cal ky BP; Fig. 2a) is only recognised in the Lake Richmond and Lake Rotokare cores, because most of the Taranaki peatlands have been drained and developed into pasture, causing oxidation, mixing and loss of the upper ~1 m of sediment. In Lake Umutekai, uncompacted suspended material at the top of the sediment core was lost during extraction (Turner 2008). HRTD interval-1 is preceded by a distinct period of ~700 years where no tephra deposition is observed (A; Fig. 2b).

The HRTD interval-2 (~2 cal ky BP) is recognised in all sediment cores, but is most prominent within the Lake Richmond record (0.028 units per year; Fig. 2a). HRTD interval-2 was generated by eruptions from two vents, mafic eruptions from Fanthams Peak (1966 m elevation on the southern flanks of the volcano) producing the Manganui tephras, which intercalate with more silicic units (e.g. Maketawa tephras) from the summit vent of the 2518 m Mt. Taranaki (Damaschke et al. 2017b; Torres-Orozco et al. 2017). The preceding HRTD interval-3 (~3.5 cal ky BP) only encompasses tephras from the summit vent, including the prominent and widespread Inglewood tephra unit. It is noteworthy that the HRTD intervals-2 and -3 within the Lake Rotokare record contain tephras that are ~300–500 years older than their apparent age determinations of their tephra correlatives (Fig. 2a).

The HRTD interval-4 (~5 cal ky BP; Fig. 2a) is best observed within the Lake Richmond and Lake Umutekai cores, because during this time interval discontinuous peat accumulation hindered complete tephra preservation within the peat

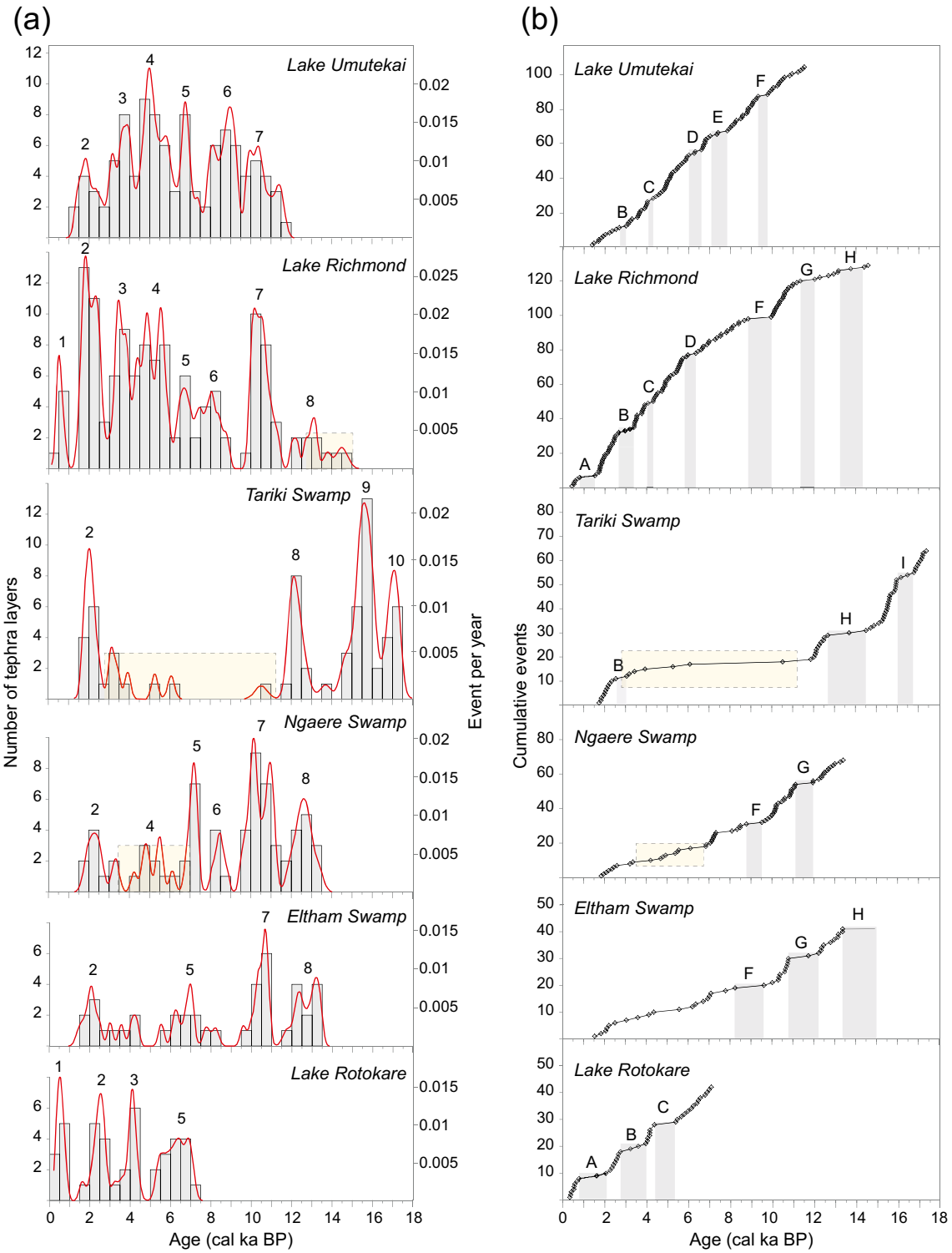

Fig. 2 **a** The rates of deposition of tephras within lake and peat sequences recovered from six different localities at Mt. Taranaki (age data from Damaschke et al. 2017a) presented as histograms of tephras deposited over 500-year intervals (left axis, grey columns), and annual tephra deposition rates generated using a Gaussian kernel smoother (Silverman 1984, 1986; Wand and Jones 1994) with a 100-year bandwidth (right axis, red line). Numbers indicate intervals during which particularly high rates of tephra deposition occurred. **b** Cumulative deposition of the same tephra units. Letters indicate periods of low rates of tephra deposition and/or no deposition. Yellow coloured fields represent disturbed or oxidised/dried sediment horizons

records. The HRTD interval-5 (~ 7 cal ky BP; Fig. 2a), however, is also prominent within the Ngaere Swamp, and so expands the length of this phase of high rates of tephra deposition to ~ 1000 years. The preceding HRTD interval-6 (~

8.5 cal ky BP; Fig. 2a) is most prominent within Lake Umutekai and preserves tephra layers not recognised/preserved within the rest of the tephra records (i.e. U-78 to U-87, ~ 9–9.4 cal ky BP; Damaschke et al. 2017a).

The HRTD interval-7 (~ 10.5 cal ky BP; Fig. 2a) is noted within most records, except Tariki Swamp (section of disturbed sediment), and it is too old for Lake Rotokare. A tephra deposition rate of up to 0.02 units per year is recorded for this interval. The HRTD interval-8 (~12.5 cal ky BP; Fig. 2a) appears to be time-transgressive (e.g. Tariki Swamp vs. Ngaere Swamp). This probably results from large age errors, because a distinctive geochemical fingerprint of this tephra sequence allows its correlation between sites. The HRTD interval-8 is separated from HRTD interval-9 (~ 15 cal ky BP) by a period of non-tephra deposition lasting > 500 years (H; Fig. 2b). The HRTD intervals-9 and -10 (~ 17 cal ky BP) are only documented within the Tariki Swamp tephra record, because none of the other sequences contained recognisable tephras in this time interval.

It is clear from these data that multiple tephra records can help to construct a more robust and complete eruption record from a volcano. Site-specific gaps, overlaps and/or offsets in the rate of tephra deposition can be recognised between locations. However, it must be remembered that, although this NE-SE sampling arc is downwind for the prevailing winds, it covers only about 120° around the eastern side of the volcano and is likely missing eruptive events dispersed to the unfavourable upwind direction to the south and west, as well as effusive eruptions with minor or no associated falls. Hence, the frequency data remain an underrepresentation of the true volcanism and any synthesis of them is only a minimum-estimate of reality. Methods of combining multiple eruption deposits and sequences into a single record of eruption events are described below.

Merging tephra records

A first-order composite stratigraphic record was created by conventional manual merging of core segments based on distinctive appearance or properties of individual tephras or sequences of them, reinforced by distinct geochemical tephra sequences (Damaschke et al. 2017a). This 'composite manual' stratigraphy includes ~ 228 tephras, spanning the last 30 cal ky BP. The quality of this record varies, with the older part contained within only one core and being compromised by a large break in deposition. As a first-order estimate of eruption frequency, this composite record is most reliable only in the post-17.5 cal ky BP part. This partial record includes ~ 189 tephra layers with an average interval between eruptions of 92 years (0.011 tephra deposition events per year, Fig. 3a).

A second means of merging tephra sequences applied the Green et al. (2014) matching algorithm, based on interpolated age determinations of tephra layers at each site, with the stratigraphic-order at each site fixed, and geochemical compositions used to force (or exclude) specific tephra matches. Due to the stratigraphic constraints of the process, well-matched tephras produce flow-on consequences to correlations of units stratigraphically above or below them. For this dataset, the resulting statistically combined record comprises ~ 272 tephra layers spanning the last 30 cal ky BP, including ~ 231 tephra layers within the continuous sequences younger than 17.5 cal ky BP (Fig. 3b). The latter implies an average ashfall frequency of one event per 75 years (0.013 tephra deposition events per year).

The composite manual approach provided an underestimate of event frequency, because it cobbles-together blocks of tephra sequences at individual sites, and this mostly avoids any possibility of doubling-up closely timed events. Where strong winds prevail (common in New Zealand), tephras may be dispersed in very narrow lobes (e.g. Ruapehu 1995 and 1996 eruptions, Cronin et al. 2003; Te Maari eruption 2012; Turner et al. 2014). Hence, a single site will never capture a record of all eruptions. A good example of this is at ~ 4.3 cal ky BP, where the 'best-core' record is a segment of the Lake Umutekai sequence that misses tephras seen at Lake Richmond (C; Fig. 3a). This gap is ameliorated within the statistically combined record (Fig. 3b).

Using a piecewise cubic Hermitian interpolating polynomial (Fritsch and Carlson 1980) to develop an age model for each sediment record, uncertainties vary down-core depending on the intervals between dates and the curvature of the fitted polynomial. Thus, sudden changes in sediment accumulation rate and unconformities may blurred in the resulting age-depth relationships (Telford et al. 2004; Blaauw 2010). Comparing cores, there is an apparent temporal offset of HRTD intervals-2 and -3 in the Lake Rotokare record, compared to the rest of the frequency records (Figs. 2 and 4). Geochemical compositions of the glass, titanomagnetite grains and whole-lapilli samples show however that these horizons should be correlated (Damaschke et al. 2017a). Thus, the depositional ages in the Lake Rotokare record are inaccurate. At least one of the ^{14}C determinations for this site may have been contaminated by an old carbon effect (e.g. Keaveney and Reimer 2012; Philippsen 2013; Hart 2014). Lake Rotokare is unique amongst the sites studied here in being a landslide-dammed lake within a steep valley set in strongly eroding Tertiary-aged calcareous mudstone and sandstone. Turner (2008) noted frequent landslide deposition into this lake, and the tephra layers are intercalated with the mud-rich landslide debris. The age inconsistencies meant that the Lake Rotokare tephra ages could not be used directly within the statistical matching process, without detailed in-core correlation adjustments. Due to the multiple age inconsistencies, such corrections would have needed additional overlapping core coverage to avoid potentially circular logic in the adjustments. We thus omitted a potentially complex

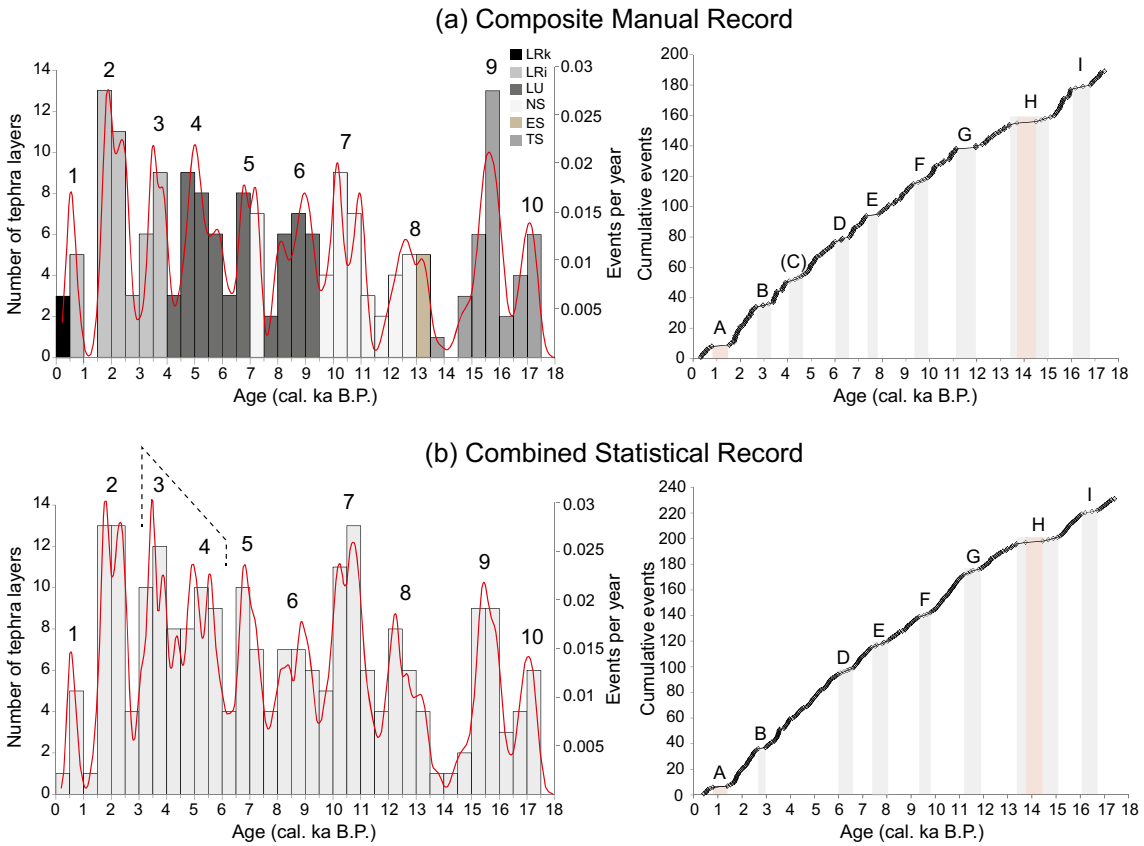

Fig. 3 Variation in the deposition rate of tephra layers across all sites analysed presented as histograms of tephras deposited over 500-year intervals (left axis, columns), and annual tephra deposition rates generated using a Gaussian kernel smoother (Silverman 1984, 1986; Wand and Jones 1994) with a 100-year bandwidth (right axis, red line). Cumulative deposition rates are also shown. Two different matching models are presented: **a** A manually merged composite record with conservative traditional stratigraphic matching, based on tephra appearance (individual and patterns) and geochemical matches; and **b** a statistically combined record developed using a matching algorithm (following the approach of Green et al. 2014). Numbers indicate periods of high rates of tephra deposition and letters indicate periods where tephra deposition rates were low including two quiescence periods (A and H; marked as red-shaded fields) (refer to text). Note: HRTD intervals-3 and -4 may indicate one long-lasting high-frequency interval, since no repose times > 200 years are recorded within this particular period (dotted line). *LRk* Lake Rotokare, *LRi* Lake Richmond, *LU* Lake Umutekai, *NS* Ngaere Swamp, *ES* Eltham Swamp, *TS* Tariki Swamp

site-correction in this study, and subsequently excluded the Lake Rotokare record from further statistical matching procedures.

Highly variable background sedimentation regimes may also disrupt statistical merging procedures, as observed for certain horizons within the Tariki Swamp record (Figs. 2 and 4). In parts of this sequence, thick silt loam horizons occur, in which tephra deposits are diffuse and possibly reworked (Damaschke et al. 2017a). Consequently, age determinations may be biased, and have large error ranges that add disruptive 'noise' to the matching procedure. For this reason, the affected part of the Tariki Swamp record (e.g. 3–12 cal ky BP) was also excluded from further statistical matching.

Past studies have shown that additional geochemical data can provide valuable constraints within a statistical matching procedure (Turner et al. 2009; Green et al. 2014). These data can be used to prevent matches with incompatible compositions, and also force some that are obviously distinctive (Damaschke et al. 2017a; Table 2), over-riding and correcting temporal positioning. The composition of mineral, glass and whole-rock samples from many andesitic volcanoes rarely allow unique correlations (e.g. Cronin et al. 1996). Therefore, only a few geochemically fixed points (Table 2) were applied. Using these, we derived the most robust statistically combined record yet for Mt. Taranaki eruptions (Figs. 3b and 4).

Irrespective of the merging method, all records of eruption here and in earlier studies (Turner et al. 2008, 2009, 2011b) show a similar pattern of cyclic variation in eruption frequency over time at Mt. Taranaki (Fig. 3a, b). Our new data defines ten periods of high tephra deposition/eruption frequency, each ~ 1000–1500 years in duration. These are separated by eight periods of low eruption frequency, including two intervals of > 500 years with no tephra deposition (A and H, centred on ~ 1 and ~ 14 cal ky BP, respectively; Fig. 3a, b), which may indicate two significant quiescence periods at Mt. Taranaki.

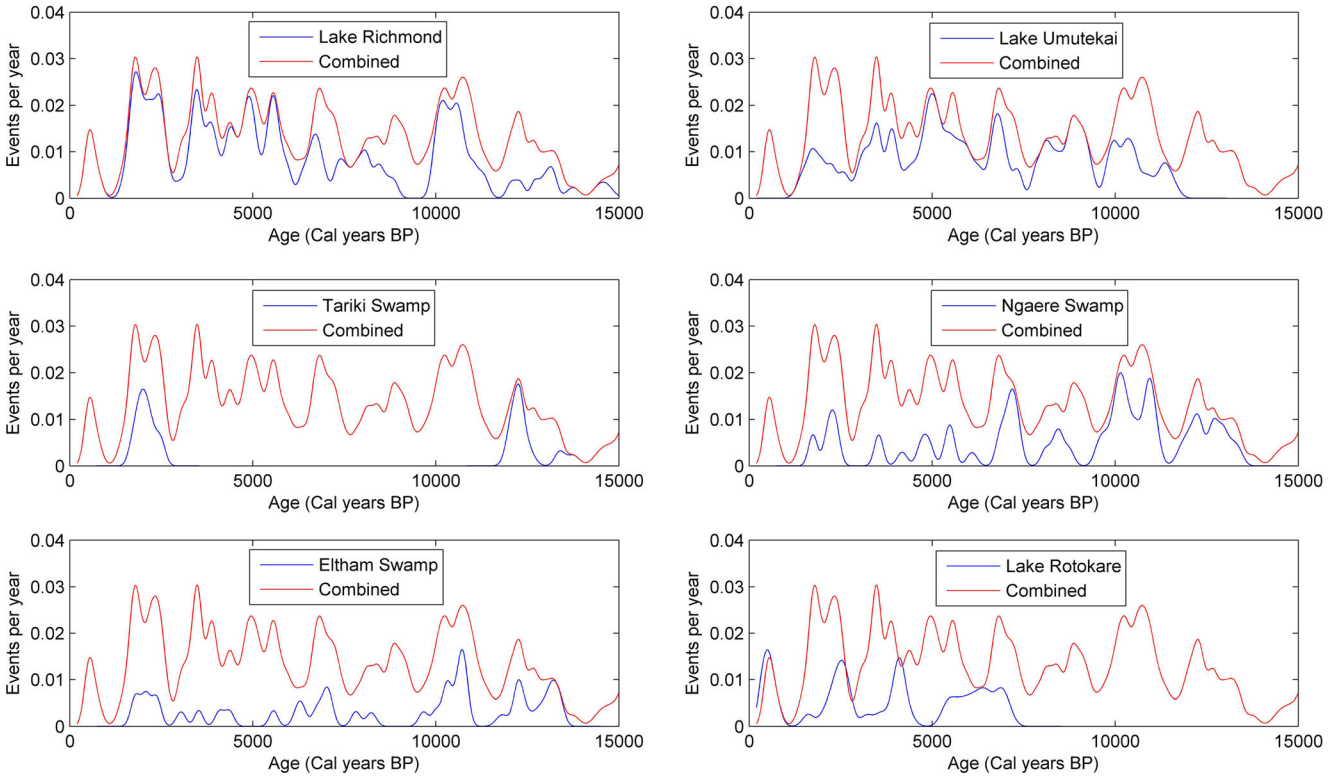

Fig. 4 Annual tephra deposition rates of each single record in comparison with the statistically combined record. Rates are generated using a Gaussian kernel smoother (Silverman 1984, 1986; Wand and Jones 1994) with a 100-year bandwidth. Note the offset of the Lake Rotokare events

On the other hand, two of the HRTD intervals-3 and -4 (from 6 to 3 cal ky BP) are so close together that they could be considered a single continuous high-activity period, since no > 200-year. repose intervals occur (Fig. 3b). Over this 3000-year period, the average interval between ashfalls is 52 years (0.019 events per year).

Probabilistic modelling

Forecasting of a future tephra-producing eruption was carried out using the final statistically combined tephra dataset for < 14.5 cal ky BP events using: (1) the exponential distribution (Poisson process), (2) the Weibull renewal and (3) the mixture of Weibull renewal models. The Tahurangi eruption, dated by dendrochronology at AD1755, is the last recorded significant tephra fall (Druce 1966). However, the summit dome was emplaced and partly collapsed after this in the Sisters eruption. In the absence of reliable radiocarbon dating, Platz et al. (2012) estimated this last eruption of Mt. Taranaki occurred between AD1785 and AD1820. This age range was incorporated as the last event in the forecasting model.

The estimated parameters and average log likelihoods for each model are shown in Table 3. In total, 200 events span the last ~ 14.5 cal ky BP in our final record. A Monte Carlo simulation was run with $n = 100$ (i.e. 19,900 sampled inter-event times) to derive the fitted densities shown in Fig. 5. In an update from previous procedures (Turner et al. 2008, 2009), this study used calibrated calendar ages applying OxCal Version 4.2 (Bronk Ramsey 2013) and the Southern Hemisphere SHCal13 atmospheric calibration curve (Hogg et al. 2013).

The best fit for the distribution of modelled inter-event periods was achieved by the mixture of the Weibull model according to the AIC statistic (Table 3). The Poisson process is less well suited, because event times are systematically variable. The Weibull renewal distribution has $\alpha < 1$ implying clustering behaviour. In this case, α is almost = 1; thus, the result is very similar to a simple Poisson process (indicated by the dotted and dashed lines almost overlying (Figs. 5 and 6). The mixtures distribution includes a strong primary mode at inter-event times of ~ 9 years and a secondary mode at inter-event times of ~580 years (Table 3). The overall pattern is similar in form to that in an earlier work (Turner et al. 2008, 2009), but with a much more refined outcome, indicated by increased α and p values (with $p = 1$ corresponding to a simple unimodal Weibull distribution; Table 3). The primary short-repose mode (mean repose ~ 65 years) now accounts for 98% of interval times, while the secondary long repose mode reduces to only 2% compared to 25–4% in previous studies. The long repose mode is also longer at ~ 580 years compared to ~ 165 and ~ 210 years in a previous work (Turner et al. 2008, 2009; Fig. 7b). This implies that activity at Mt. Taranaki is

Table 2 Correlation pairs used in the merging algorithm (c.f., Green et al. 2014). They are based on the physical and geochemical characteristics of the tephras, as well as, on their stratigraphic position and age constraints (implemented by Damaschke et al. 2017a)

Correlation pairs	Lake Umutekai	Lake Richmond	Tariki Swamp	Ngaere Swamp	Eltham Swamp
1	U-4	Ri-10			
2				N-2	E-1
3				N-6	E-5
4		Ri-26	T-10	N-7	E-6
5	U-20	Ri-40		N-8	E-8
6	U-25	Ri-47			
7	U-34	Ri-60			
8	U-39	Ri-65			
9	U-60	Ri-84			
10				N-42	E-23
11		Ri-113		N-46	
12		Ri-121	T-21	N-57	
13			T-23	N-58	E-32
14			T-29	N-68	E-41

overall more frequent than previously detected, but there are better defined long breaks where tephra-producing eruptions are not occurring.

The probability of no eruption in the next t years, given that the most recent event occurred at T years ago, is:

$$\Pr(\tau > T + t | \tau > T) = \frac{\int_{T+t}^{\infty} f(\tau) d\tau}{\int_{T}^{\infty} f(\tau) d\tau}. \quad (7)$$

Assuming that the last eruption event occurred between AD1785 and AD1820, the probability of an eruption within the next 50 years is 33–42%, based on the best fitting mixture of the Weibull model (Fig. 6a). This is significantly lower than previous probability models using only two records, which suggested a 52–59% chance of eruption within the next 50 years (Turner et al. 2009; Fig. 7a). Plotting the annual eruption probability progression (Fig. 6b), the preferred mixture of the Weibull model indicates that a high-probability peak occurred at approximately AD1900 (annual eruption probability of ~0.016 or 1.6%) and this will decline to a trough at ~AD2200 (annual eruption probability of ~0.003 or 0.3%). The current annual eruption probability is estimated at 0.01 to 0.013 (1 to 1.3%; Fig. 6b). This indicates that the likelihood of a long repose is steadily increasing with a steady decrease in the annual probability of a future eruption within the short to medium term future.

These results contrast strongly with previous estimates made by Turner et al. (2009) (Fig. 7), who estimated a current annual eruption rate of 0.016 (1.6%) with the trough occurring earlier (i.e. after 210 years in the two-core merged record). This subtle difference in the secondary mode of inter-event times strongly affects the eruption probability progression of Turner et al. (2008, 2009) compared to our update (Fig. 7b). Part of the reason for this is that Turner et al. (2009) used the Lake Rotokare record to fill potential gaps within the Lake Umutekai record. However, as revealed in here, the Lake Rotokare record is strongly, but non-systematically, biased in its age estimates. This led to an apparent infill of long intervals, and possibly an inflation of the true tephra fall frequency, and the differences in forecast results described above.

Table 3 Fitted parameters and average log likelihoods for the models tested for both of the last explosive eruptions of Mt. Taranaki at AD1785 and AD1820

Model	Last event AD1785				Last event AD1820			
	Parameters	Modes	logL	AIC	Parameters	Modes	logL	AIC
Poisson process	$\lambda = 0.0134$	0	− 1046.4	2094.7	$\lambda = 0.0134$	0	− 1046.4	2094.7
Weibull renewal process	$\alpha = 0.9901$ $\beta = 0.0136$	0	− 1044.1	2092.2	$\alpha = 0.9922$ $\beta = 0.0136$	0	− 1043.6	2091.2
Mixture of Weibull renewal process	$\alpha_1 = 1.1206$ $\beta_1 = 0.0147$ $\alpha_2 = 3.7393$ $\beta_2 = 0.0016$ $p = 0.9819$	9.31 573.70	− 1037.8	2085.5	$\alpha_1 = 1.1188$ $\beta_1 = 0.0147$ $\alpha_2 = 3.9236$ $\beta_2 = 0.0016$ $p = 0.9834$	9.20587.00	− 1037.4	2084.7

AIC Akaike Information Criterion (Akaike 1977), *logL* log-likelihood

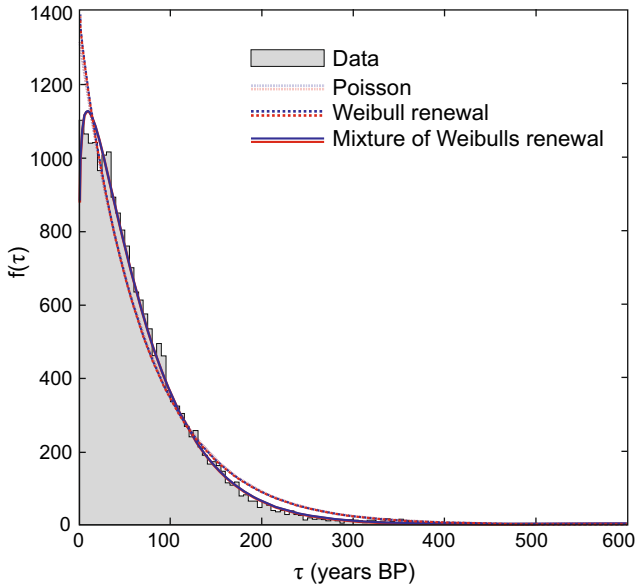

Fig. 5 Histogram of 19,900 sampled inter-event times based on Monte Carlo simulations of the new statistically combined Mt. Taranaki eruption record. Curves show the different densities fitted for this dataset with AD1785 (red) and AD1820 (blue) as last volcanic activity events

Discussion

Long and complete chronological eruption records from volcanoes are fundamental to robust probabilistic hazard models (e.g. Scandone et al. 1993, 2008; Behncke and Neri 2003; Turner et al. 2008, 2009). In this case, tephra deposition in a series of lake and peat bog sequences in a 120° downwind arc was used as a proxy for eruptions. It is clear that this sampling net will miss tephra dispersed in other, less-common wind directions, small-scale eruptions with only proximal deposits and effusive-only events. Putting this limitation aside, tephra-forming eruptions are hazardous to surrounding populations and tracking at least this type and scale of volcanism is a good way of understanding overall volcanic behaviour.

To build robust tephra records at any volcano, methods to extend from single-site to multiple-location stratigraphy are needed to capture a range of possible tephra dispersal directions, variations in eruption sizes/styles, and account for variable tephra preservation issues. Good age determinations for tephras rely strongly on a stable sedimentation background regime. In this study, one of the sites (Lake Rotokare) was discovered to have a distinctive old-carbon effect within its radiocarbon ages. It was not possible to isolate this in previous two-record combinations (Turner et al. 2009), because cross-validation required the information from the several new sites reported here. In other sites, parts of the records are disturbed, but with enough sampling sites to bridge these gaps, a good overall coverage can be achieved through subsequent merging procedures.

It has also been confirmed in this work that incorporating geochemical constraints is far more reliable for indicating incompatible matches, rather than forcing direct match-links, although the latter enormously decrease computation time (for this exercise, on the order of 2–3 days on an Intel i7 3.4 GHz desktop). Hence, a balanced approach in the use of geochemical covariates within the statistical merging procedures is suggested. Distinct titanomagnetite compositional groups for packages of tephras identified in earlier studies (Damaschke et al. 2017a) were useful to inform some correlations, but currently the matching algorithm does not include patterns of compositions, only single tephra compositions. Additional independent tools are needed to improve the correlation of tephras between multiple sites.

Probabilistic assessments of volcanic recurrence at other volcanic sites have been carried out, but due to the greater difficulties of assembling a complete record at polygenetic volcanoes, many studies have focussed on monogenetic volcanic

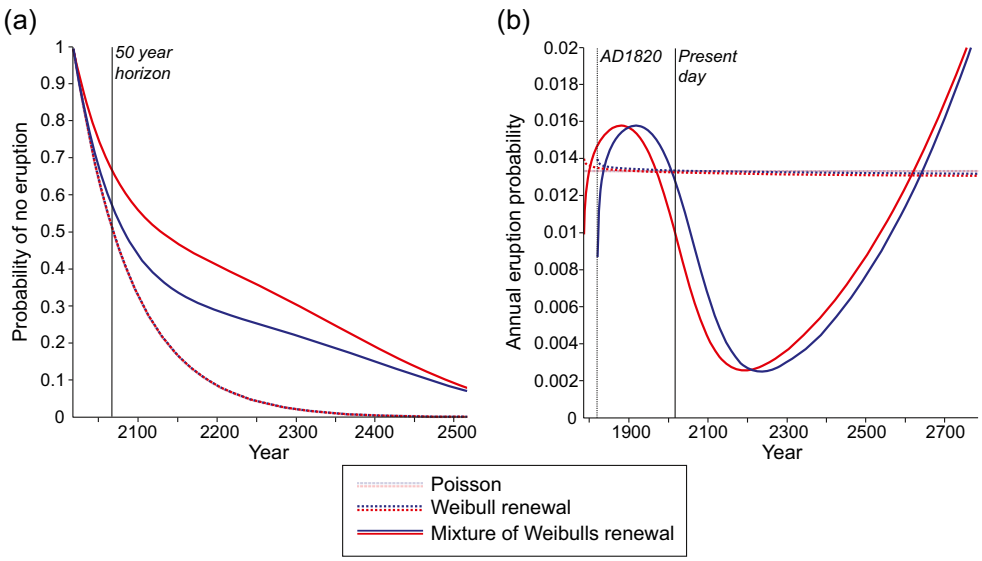

Fig. 6 **a** Probabilities of no eruption of Mt. Taranaki occurring over future time periods, based on three models of inter-event distributions with AD1785 (red) and AD1820 (blue) as last volcanic activity events. **b** Annual eruption probabilities estimated for Mt. Taranaki, assuming the last volcanic activity event was at AD1785 (red) and AD1820 (blue). The Weibull renewal distribution is similar to a simple Poisson process

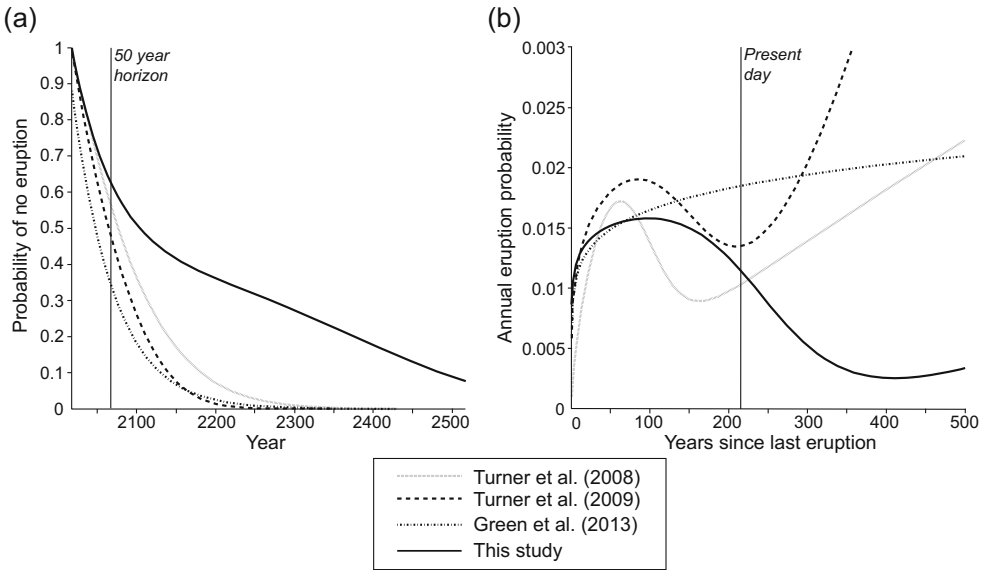

Fig. 7 **a** Probabilities of no eruption at Mt. Taranaki occurring over future time periods, based on the inter-event distribution constructed in each previous paper and for the statistically combined record built in this study, with AD1800 (compromise date between AD1785 and AD1820) as the last volcanic event. **b** Annual eruption probabilities of Mt. Taranaki estimated for different records proposed in previous studies and for the statistically combined record built in this study, assuming the last volcanic event was at AD1800

fields and caldera or rift-zone volcanoes (e.g. Yucca Mountain region, Connor and Hill 1995; Ho and Smith 1997, 1998; Connor et al. 2000; Springerville volcanic field, Arizona, Condit and Connor 1996; Taveuni volcano, Fiji, Cronin et al. 2001; Auckland volcanic field, Molloy et al. 2009; Bebbington and Cronin 2011; Campi Flegrei caldera, Orsi et al. 2009, Bevilacqua et al. 2016). These tend to have a far more erratic temporal variation compared to long-lived subduction-related stratovolcanoes. However, Wadge (1982) conjectured that stratovolcanoes may exhibit periods of high-frequency activity interspersed by longer periods of quiescence.

Many studies (e.g. Klein 1982; De la Cruz- Reyna 1993; Behncke and Neri 2003; Cappello et al. 2013) of eruption forecasting have been made using historical data, which often means short (c. 200–400 year) eruption records at individual volcanoes. A number of these cases were shown to exhibit cyclic patterns on the order of decades to centuries (Bebbington 2010). Another longer, relatively complete, record is Mt. Vesuvius (Scandone et al. 1993, 2008), which shows a well-defined eruption cycle, where each cycle is initiated (or ended) by a large (sub-Plinian to Plinian) eruption, similar to the behaviour of Mt. Taranaki postulated by Turner et al. (2011b).

According to the present study, Mt. Taranaki exhibits strong cyclic patterns in event frequency, with an apparent long secondary mode in the repose time distribution, which may have implications for the details of its magmatic system. Those longer inter-event intervals may correspond to less-frequent feeding pulses of magma replenishment to lower-mid crustal storage systems between bursts of rapid supply/replenishment rates (Turner et al. 2011b). The cycles may also be linked with distinct tectonic regime processes, such as changes in the regional crustal stress, enabling magma movement and accommodation in the crust (cf., Walter et al. 2007; Watt et al. 2009; Caricchi et al. 2014). Regular gravitational loading and unloading of the volcano due to regular collapse and re-growth cycles as seen at Mt. Taranaki (Zernack et al. 2012) may also modify the stress-field enough to suppress or enhance magma ascent rates and/or dyke propagation (e.g. Pinel and Jaupart 2000; Muller et al. 2001; McGovern et al. 2013). Suppression phases could lead to periods of low-activity and be terminated due to unloading of the volcano by large debris avalanche events (Manconi et al. 2009; Pinel and Albino 2013). At Mt. Taranaki two major debris avalanches occurred during the time frame investigated in this study, the ~14 cal ky BP Motumate debris avalanche, and the ~7.5 cal ky BP Opua debris avalanche (Zernack et al. 2011). It is unclear if the earlier collapse had any influence, because it is at the beginning of the robust combined record. The window of the 7.5 cal ky BP terminating growth/collapse cycle is, however, captured in the new record, but clear pre/post-collapse variability is not immediately obvious, because shorter-period variability dominates this time frame.

Conclusions

This study has shown how important it is to assemble as large a number of independent records of eruption frequency as possible, in this case from high-sensitivity tephra deposition sites. The large number of sites allow potentially anomalous records to be identified (e.g. when dating is erroneous or deposition rates are too irregular). Adding additional stratigraphic records to such studies comes with the added complexity, however, of the need to find reliable means to combine and merge individual sequences to create a robust overall eruption record for modelling. Here, we conclude that applying statistical methods that compare age-error models between deposition sites, within a rigid stratigraphic requirement, is a first step. Adding geochemical constraints to this, in terms of direct

layer correlations or by enabling exclusion of potential matches based on composition, can markedly improve the reliability of the process. Future work is needed to incorporate less well-defined geochemical criteria, such as the identification of temporal chemical groupings, as is seen at Mt. Taranaki. In addition, incorporation of proximal data and understanding missing elements of individual eruption records are needed.

Based on the best model yet for Mt. Taranaki, we estimate there is a 33–42% probability of an eruption occurring within the next 50 years. This is a reduction in likelihood compared to a previous work. The new record and model provide strong evidence that Mt. Taranaki is currently within a 'long' repose. We confirm that there is a cyclicity in eruption frequency over time at Mt. Taranaki, which was proposed in previous studies. There is one unusual double-period, however, between 3 to 6 cal ky BP, where there is highly frequent volcanism with no repose periods longer than 200 years. Understandings of the drivers behind this remain unclear, although it may relate to the aftermath of the latest debris avalanche from this volcano.

The principles applied here can be implemented at any similar 're-awakening' volcano. It is thus important to build such high-resolution records at other sites in order to test whether cyclic variations in eruption frequency and bimodal distributions of inter-event times are a characteristic feature of andesitic stratovolcanoes.

Acknowledgements MD acknowledges the support of a Massey University Doctoral Scholarship, and an Auckland University supplementary scholarship. MD also would like to thank Prof Clel Wallace (Massey University) for thorough review of this manuscript. SJC and MB are supported by the NZ Natural Hazards Research Platform project, 'Quantifying exposure to specific and multiple volcanic hazards'. We thank Roberto Sulpizio and an unnamed reviewer along with editor Laura Sandri for their excellent suggestions on our original manuscript.

References

Akaike H (1977) An extension of the method of maximum likelihood and the Stein's problem. Ann Inst Stat Math 29(1):153–164. https://doi.org/10.1007/BF02532781

Alloway BV, Neall VE, Vucetich CG (1995) Late Quaternary (post 28, 000 year BP) tephrostratigraphy of northeast and central Taranaki, New Zealand. J Roy Soc New Zeal 25(4):385–458. https://doi.org/10.1080/03014223.1995.9517496

Alloway BV, McComb P, Neall VE, Vucetich C, Gibb J, Sherburn S, Stirling M (2005) Stratigraphy, age, and correlation of voluminous debris-avalanche events from an ancestral Egmont Volcano: implications for coastal plain construction and regional hazard assessment. J Roy Soc New Zeal 35(1–2):229–267. https://doi.org/10.1080/03014223.2005.9517782

Andreastuti SD, Alloway BV, Smith IEM (2000) A detailed tephrostratigraphic framework at Merapi Volcano, Central Java, Indonesia: implications for eruption predictions and hazard assessment. J Volcanol Geoth Res 100(1):51–67. https://doi.org/10.1016/S0377-0273(00)00133-5

Bebbington MS (2010) Trends and clustering in the onsets of volcanic eruptions. J Geophys Res: Sol Ea 115(B1). https://doi.org/10.1029/2009JB006581

Bebbington MS, Lai CD (1996a) On nonhomogeneous models for volcanic eruptions. Math Geol 28(5):585–600. https://doi.org/10.1007/BF02066102

Bebbington MS, Lai CD (1996b) Statistical analysis of New Zealand volcanic occurrence data. J Volcanol Geoth Res 74(1):101–110. https://doi.org/10.1016/S0377-0273(96)00050-9

Bebbington MS, Cronin SJ (2011) Spatio-temporal hazard estimation in the Auckland Volcanic Field, New Zealand, with a new event-order model. B Volcanol 73(1):55–72. https://doi.org/10.1007/s00445-010-0403-6

Behncke B, Neri M (2003) Cycles and trends in the recent eruptive behaviour of Mount Etna (Italy). Can J Earth Sci 40(10):1405–1411. https://doi.org/10.1139/e03-052

Bevilacqua A, Flandoli F, Neri A, Isaia R, Vitale S (2016) Temporal models for the episodic volcanism of Campi Flegrei caldera (Italy) with uncertainty quantification. Journal of Geophysical Research: Solid Earth 121(11):7821–7845

Blaauw M (2010) Methods and code for 'classical' age-modelling of radiocarbon sequences. Quat Geochronol 5(5):512–518. https://doi.org/10.1016/j.quageo.2010.01.002

Boudt K, Caliskan D, Croux C (2011) Robust explicit estimators of Weibull parameters. Metrika 73(2):187–209. https://doi.org/10.1007/s00184-009-0272-1

Bronk Ramsey C (2013) OxCal 4.2. Web Interface Build (78)

Bursik M (1998) Tephra dispersal. Geol Soc Spec Publ 145(1):115–144. https://doi.org/10.1144/GSL.SP.1996.145.01.07

Cappello A, Bilotta G, Neri M, Negro CD (2013) Probabilistic modeling of future volcanic eruptions at Mount Etna. Journal of Geophysical Research: Solid Earth 118(5):1925–1935

Carey S, Sparks RSJ (1986) Quantitative models of the fallout and dispersal of tephra from volcanic eruption columns. B Volcanol 48(2–3):109–125. https://doi.org/10.1007/BF01046546

Caricchi L, Annen C, Blundy J, Simpson G, Pinel V (2014) Frequency and magnitude of volcanic eruptions controlled by magma injection and buoyancy. Nat Geosci 7(2):126–130. https://doi.org/10.1038/ngeo2041

Condit CD, Connor CB (1996) Recurrence rates of volcanism in basaltic volcanic fields: an example from the Springerville volcanic field, Arizona. Geol Soc Am Bull 108(10):1225–1241. https://doi.org/10.1130/0016-7606(1996)108<1225:RROVIB>2.3.CO;2

Connor CB, Hill BE (1995) Three nonhomogeneous Poisson models for the probability of basaltic volcanism: application to the Yucca Mountain region, Nevada. J Geophys Res: Sol Ea 100(B6):10107–10125. https://doi.org/10.1029/95JB01055

Connor CB, Stamatakos JA, Ferrill DA, Hill BE, Ofoegbu GI, Conway FM, Sagar B, Trapp J (2000) Geologic factors controlling patterns of small-volume basaltic volcanism: application to a volcanic hazards assessment at Yucca Mountain, Nevada. J Geophys Res: Sol Ea 105(B1):417–432. https://doi.org/10.1029/1999JB900353

Cronin SJ, Neall VE, Stewart RB, Palmer AS (1996) A multiple-parameter approach to andesitic tephra correlation, Ruapehu volcano, New Zealand. J Volcanol Geoth Res 72(3):199–215. https://doi.org/10.1016/0377-0273(96)00008-X

Cronin SJ, Bebbington MS, Lai C (2001) A probabilistic assessment of eruption recurrence on Taveuni volcano, Fiji. B Volcanol 63(4):274–288. https://doi.org/10.1007/s004450100144

Cronin SJ, Neall VE, Lecointre JA, Hedley MJ, Loganathan P (2003) Environmental hazards of fluoride in volcanic ash: a case study from Ruapehu volcano, New Zealand. J Volcanol Geoth Res 121(3):271–291. https://doi.org/10.1016/S0377-0273(02)00465-1

Damaschke M, Cronin SJ, Holt KA, Bebbington MS, Hogg AG (2017a) A 30,000 yr high-precision eruption history for the andesitic Mt. Taranaki, North Island. New Zealand Quaternary Res 87(1):1–23

Damaschke M, Cronin SJ, Torres-Orozco R, Wallace RC (2017b) Unifying tephrostratigraphic approaches to redefine major Holocene marker tephras, Mt. Taranaki, New Zealand. J Volcanol Geoth Res 337:29–43. https://doi.org/10.1016/j.jvolgeores.2017.02.021

Dartevelle S, Ernst GG, Stix J, Bernard A (2002) Origin of the Mount Pinatubo climactic eruption cloud: implications for volcanic hazards and atmospheric impacts. Geol 30(7):663–666. https://doi.org/10.1130/0091-7613(2002)030<0663:OOTMPC>2.0.CO;2

De la Cruz-Reyna S (1991) Poisson-distributed patterns of explosive eruptive activity. B Volcanol 54(1):57–67. https://doi.org/10.1007/BF00278206

De la Cruz-Reyna S (1993) Random patterns of occurrence of explosive eruptions at Colima Volcano, Mexico. J Volcanol Geotherm Res 55(1–2):51–68

Donoghue SL, Vallance J, Smith IE, Stewart RB (2007) Using geochemistry as a tool for correlating proximal andesitic tephra: case studies from Mt Rainier (USA) and Mt Ruapehu (New Zealand). J Quaternary Sci 22(4):395–410. https://doi.org/10.1002/jqs.1065

Druce AP (1966) Tree-ring dating of recent volcanic ash and lapilli, Mt Egmont. New Zeal J Bot 4(1):3–41. https://doi.org/10.1080/0028825X.1966.10443951

Dzierma Y, Wehrmann H (2010) Eruption time series statistically examined: probabilities of future eruptions at Villarrica and Llaima Volcanoes, Southern Volcanic Zone, Chile. J Volcanol Geoth Res 193(1):82–92. https://doi.org/10.1016/j.jvolgeores.2010.03.009

Fritsch FN, Carlson RE (1980) Monotone piecewise cubic interpolation. SIAM J Numer Anal 17(2):238–246. https://doi.org/10.1137/0717021

Gaillard JC (2006) Traditional societies in the face of natural hazards: the 1991 Mt. Pinatubo eruption and the Aetas of the Philippines. Int J Mass Emerg Disast 24(1):5–43

Garcia-Aristizabal A, Marzocchi W, Fujita E (2012) A Brownian model for recurrent volcanic eruptions: an application to Miyakejima volcano (Japan). Bull Volcanol 74(2):545–558. https://doi.org/10.1007/s00445-011-0542-4

Green RM, Bebbington MS, Cronin SJ, Jones G (2014) Automated statistical matching of multiple tephra records exemplified using five long maar sequences younger than 75ka, Auckland, New Zealand. Quat Res 82(2):405–419. https://doi.org/10.1016/j.yqres.2014.06.004

Hart JP (2014) A model for calculating freshwater reservoir offsets on AMS-dated charred, encrusted cooking residues formed from varying resources. Radiocarbon 56(3):981–989. https://doi.org/10.2458/56.17558

Ho CH, Smith EI (1997) Volcanic hazard assessment incorporating expert knowledge: application to the Yucca Mountain region, Nevada, USA. Math Geol 29(5):615–627. https://doi.org/10.1007/BF02769647

Ho CH, Smith EI (1998) A spatial-temporal/3-D model for volcanic hazard assessment: application to the Yucca Mountain region, Nevada. Math Geol 30(5):497–510. https://doi.org/10.1023/A:1021785910495

Hogg AG, Hua Q, Blackwell PG, Niu M, Buck CE, Guilderson TP, Heaton TJ, Palmer JG, Reimer PJ, Reimer RW, Turney CSM, Zimmerman SRH (2013) SHCal13 Southern Hemisphere calibration, 0-50,000 years cal BP. Radiocarbon 55(04):1889–1903. https://doi.org/10.2458/azu_js_rc.55.16783

Jiang R, Murthy DNP (1995) Reliability modeling involving two Weibull distributions. Reliab Eng Syst Safe 47(3):187–198. https://doi.org/10.1016/0951-8320(94)00045-P

Jiang R, Murthy DNP (1998) Mixture of Weibull distributions—parametric characterization of failure rate function. Appl Stoch Model Data Anal 14(1):47–65. https://doi.org/10.1002/(SICI)1099-0747(199803)14:1<47::AID-ASM306>3.0.CO;2-E

Johnston DM, Houghton BF, Neall VE, Ronan KR, Paton D (2000) Impacts of the 1945 and 1995–1996 Ruapehu eruptions, New Zealand: an example of increasing societal vulnerability. Geol Soc Am Bull 112(5):720–726. https://doi.org/10.1130/0016-7606(2000)112<720:IOTARE>2.0.CO;2

Keaveney EM, Reimer PJ (2012) Understanding the variability in freshwater radiocarbon reservoir offsets: a cautionary tale. J Archaeol Sci 39(5):1306–1316. https://doi.org/10.1016/j.jas.2011.12.025

Klein FW (1982) Patterns of historical eruptions at Hawaiian volcanoes. J Volcanol Geotherm Res 12(1–2):1–35

Lowe DJ (1988) Stratigraphy, age, composition, and correlation of late Quaternary tephras interbedded with organic sediments in Waikato lakes, North Island, New Zealand. New Zeal J Geol Geophys 31(2):125–165. https://doi.org/10.1080/00288306.1988.10417765

Manconi A, Longpré MA, Walter TR, Troll VR, Hansteen TH (2009) The effects of flank collapses on volcano plumbing systems. Geol 37(12):1099–1102. https://doi.org/10.1130/G30104A.1

Marzocchi W, Bebbington MS (2012) Probabilistic eruption forecasting at short and long time scales. B Volcanol 74(8):1777–1805. https://doi.org/10.1007/s00445-012-0633-x

McGovern PJ, Rumpf ME, Zimbelman JR (2013) The influence of lithospheric flexure on magma ascent at large volcanoes on Venus. J Geophys Res: Planets 118(11):2423–2437. https://doi.org/10.1002/2013JE004455

Melnik O, Sparks RSJ (1999) Nonlinear dynamics of lava dome extrusion. Nature 402(6757):37–41. https://doi.org/10.1038/46950

Miyaji N (1988) History of younger Fuji volcano. J Geol Soc Jpn 94(6):433–452. https://doi.org/10.5575/geosoc.94.433

Molloy C, Shane P, Augustinus P (2009) Eruption recurrence rates in a basaltic volcanic field based on tephra layers in maar sediments: implications for hazards in the Auckland volcanic field. Geol Soc Am Bull 121(11–12):1666–1677. https://doi.org/10.1130/B26447.1

Muller JR, Ito G, Martel SJ (2001) Effects of volcano loading on dike propagation in an elastic half-space. J Geophys Res: Sol Ea 106(B6):11101–11113. https://doi.org/10.1029/2000JB900461

Orsi G, Di Vito MA, Selva J, Marzocchi W (2009) Long-term forecast of eruption style and size at Campi Flegrei caldera (Italy). Earth Planet Sci Lett 287(1–2):265–276. https://doi.org/10.1016/j.epsl.2009.08.013

Philippsen B (2013) The freshwater reservoir effect in radiocarbon dating. Heritage Sci 1(1):p1

Pinel V, Jaupart C (2000) The effect of edifice load on magma ascent beneath a volcano. Phil Trans R Soc A: Math Phys Eng Sci 358(1770):1515–1532. https://doi.org/10.1098/rsta.2000.0601

Pinel V, Albino F (2013) Consequences of volcano sector collapse on magmatic storage zones: insights from numerical modeling. J Volcanol Geoth Res 252:29–37. https://doi.org/10.1016/j.jvolgeores.2012.11.009

Platz T, Cronin SJ, Procter JN, Neall VE, Foley SF (2012) Non-explosive, dome-forming eruptions at Mt. Taranaki, New Zealand. Geomorphology 136(1):15–30. https://doi.org/10.1016/j.geomorph.2011.06.016

Press WH, Teukolsky SA, Vetterling WT, Flannery BP (1992) Numerical recipies in C: the art of scientific computing, 2nd edn. Cambridge University Press, New York

Reyment RA (1969) Statistical analysis of some volcanologic data regarded as series of point events. Pure Appl Geophys 74(1):57–77. https://doi.org/10.1007/BF00875187

Scandone R, Giacomelli L, Gasparini P (1993) Mount Vesuvius: 2000 years of volcanological observations. J Volcanol Geoth Res 58(1):5–25. https://doi.org/10.1016/0377-0273(93)90099-D

Scandone R, Giacomelli L, Speranza FF (2008) Persistent activity and violent Strombolian eruptions at Vesuvius between 1631 and 1944. J Volcanol Geotherm Res 170(3–4):167–180. https://doi.org/10.1016/j.jvolgeores.2007.09.014

Self S, Rampino MR (1981) The 1883 eruption of Krakatau. Nature 294(5843):699–704. https://doi.org/10.1038/294699a0

Shane P (2005) Towards a comprehensive distal andesitic tephrostratigraphic framework for New Zealand based on eruptions from Egmont volcano. J Quaternary Sci 20(1):45–57. https://doi.org/10.1002/jqs.897

Sheridan MF, Barberi F, Rosi M, Santacroce R (1981) A model for Plinian eruptions of Vesuvius. Nature 289(5795):282–285

Silverman BW (1984) Spline smoothing: the equivalent variable kernel method. Ann Stat 12(3):898–916. https://doi.org/10.1214/aos/1176346710

Silverman BW (1986) Density estimation for statistics and data analysis. Monogr Stat Appl Probab 60. Chapman and Hall/CRC Press

Small C, Naumann T (2001) The global distribution of human population and recent volcanism. Global Environmental Change Part B: Environ Hazards 3(3):93–109. https://doi.org/10.1016/S1464-2867(02)00002-5

Tanguy JC (1994) The 1902–1905 eruptions of Montagne Pelée, Martinique: anatomy and retrospection. J Volcanol Geoth Res 60(2):87–107. https://doi.org/10.1016/0377-0273(94)90064-7

Telford RJ, Heegaard E, Birks HJB (2004) All age–depth models are wrong: but how badly? Quaternary Sci Rev 23(1):1–5. https://doi.org/10.1016/j.quascirev.2003.11.003

Torres-Orozco R, Cronin SJ, Pardo N, Palmer AS (2017) New insights into Holocene eruption episodes from proximal deposit sequences at Mt. Taranaki (Egmont), New Zealand. B Volcanol 79(1):3. https://doi.org/10.1007/s00445-016-1085-5

Turner MB (2008) Eruption cycles and magmatic processes at a reawakening volcano, Mt. Taranaki, New Zealand. Unpublished PhD Thesis, INR, Massey University, New Zealand

Turner MB, Cronin SJ, Bebbington MS, Platz T (2008) Developing probabilistic eruption forecasts for dormant volcanoes: a case study from Mt Taranaki, New Zealand. B Volcanol 70(4):507–515. https://doi.org/10.1007/s00445-007-0151-4

Turner MB, Bebbington MS, Cronin SJ, Stewart RB (2009) Merging eruption datasets: building an integrated Holocene eruptive record for Mt Taranaki, New Zealand. B Volcanol 71(8):903–918. https://doi.org/10.1007/s00445-009-0274-x

Turner MB, Cronin SJ, Bebbington MS, Smith IE, Stewart RB (2011a) Integrating records of explosive and effusive activity from proximal and distal sequences: Mt. Taranaki, New Zealand. Quaternary Int 246(1):364–373. https://doi.org/10.1016/j.quaint.2011.07.006

Turner MB, Cronin SJ, Bebbington MS, Smith IE, Stewart RB (2011b) Relating magma composition to eruption variability at andesitic volcanoes: a case study from Mount Taranaki, New Zealand. Geol Soc Am Bull 123(9–10):2005–2015. https://doi.org/10.1130/B30367.1

Turner R, Moore S, Pardo N, Kereszturi G, Uddstrom M, Hurst T, Cronin S (2014) The use of Numerical Weather Prediction and a Lagrangian transport (NAME-III) and dispersion (ASHFALL) models to explain patterns of observed ash deposition and dispersion following the August 2012 Te Maari, New Zealand eruption. J Volcanol Geoth Res 286:437–451. https://doi.org/10.1016/j.jvolgeores.2014.05.017

Wadge G (1982) Steady state volcanism: evidence from eruption histories of polygenetic volcanoes. J Geophys Res: Sol Ea 87(B5):4035–4049. https://doi.org/10.1029/JB087iB05p04035

Walter TR, Wang R, Zimmer M, Grosser H, Lühr B, Ratdomopurbo A (2007) Volcanic activity influenced by tectonic earthquakes: static and dynamic stress triggering at Mt. Merapi. Geophys Res Lett 34(5):L05304

Wand MP, Jones MC (1994) Kernel smoothing. Monogr Stat Appl Probab 60. Chapman and Hall/CRC Press

Watt SFL, Mather TA, Pyle DM (2007) Vulcanian explosion cycles: patterns and predictability. Geol 35(9):839–842. https://doi.org/10.1130/G23562A.1

Watt SF, Pyle DM, Mather TA (2009) The influence of great earthquakes on volcanic eruption rate along the Chilean subduction zone. Earth Planet Sci Lett 277(3):399–407. https://doi.org/10.1016/j.epsl.2008.11.005

Wickman FE (1966) Repose period patterns of volcanoes: I. Volcanic eruptions regarded as random phenomena. Arkiv for Mineralogi och Geologi 4(4):291

Woods AW (1995) The dynamics of explosive volcanic eruptions. Rev Geophys 33(4):495–530. https://doi.org/10.1029/95RG02096

Zernack AV, Procter JN, Cronin SJ (2009) Sedimentary signatures of cyclic growth and destruction of stratovolcanoes: a case study from Mt. Taranaki, New Zealand. Sed Geol 220(3):288–305. https://doi.org/10.1016/j.sedgeo.2009.04.024

Zernack AV, Cronin SJ, Neall VE, Procter JN (2011) A medial to distal volcaniclastic record of an andesite stratovolcano: detailed stratigraphy of the ring-plain succession of south-west Taranaki, New Zealand. Int J Earth Sci 100(8):1937–1966. https://doi.org/10.1007/s00531-010-0610-6

Zernack AV, Cronin SJ, Bebbington MS, Price RC, Smith IE, Stewart RB, Procter JN (2012) Forecasting catastrophic stratovolcano collapse: a model based on Mount Taranaki, New Zealand. Geol 40(11):983–986. https://doi.org/10.1130/G33277.1